Molecular Biology of the Cell
Vol. 8, 1361–1375, July 1997

The Yeast Actin-related Protein Arp2p Is Required for the Internalization Step of Endocytosis

Violaine Moreau,*†‡ Jean-Marc Galan,‡§ Ginette Devilliers,§ Rosine Haguenauer-Tsapis,§ and Barbara Winsor*¶

*Institut de Biologie Moléculaire et Cellulaire-Centre National de la Recherche Scientifique, 67084 Strasbourg, France; and §Institut Jacques Monod-Centre National de la Recherche Scientifique, Université Paris VII, 75005 Paris, France

Submitted October 15, 1996; Accepted April 28, 1997
Monitoring Editor: David Botstein

The *Saccharomyces cerevisiae* actin-related protein Arp2p is an essential component of the actin cytoskeleton. We have tested its potential role in the endocytic and exocytic pathways by using a temperature-sensitive allele, *arp2–1*. The fate of the plasma membrane transporter uracil permease was followed to determine whether Arp2p plays a role in the endocytic pathway. Inhibition of normal endocytosis as revealed by maintenance of active uracil permease at the plasma membrane and strong protection against subsequent vacuolar degradation of the protein were observed in the mutant at the restrictive temperature. Furthermore, *arp2–1* cells accumulated ubiquitin-permease conjugates, formed prior to internalization. These effects were also visible at permissive temperature, whereas the actin cytoskeleton appeared to be normally polarized. The soluble hydrolase carboxypeptidase Y and the lipophilic dye FM 4–64 were targeted normally to the vacuole in *arp2–1* cells. Thus, Arp2p is required for internalization but does not play a major role in later steps of endocytosis. Synthetic lethality was demonstrated between *arp2–1* and the endocytic mutant *end3–1*, suggesting participation of Arp2p and End3p in the same process. Finally, no evidence for a major defect in secretion was apparent; invertase secretion and delivery of uracil permease to the plasma membrane were unaffected in *arp2–1* cells.

INTRODUCTION

In the budding yeast *Saccharomyces cerevisiae*, actin is found in cables running through the cytoplasm and in cortical patches (Adams and Pringle, 1984) that have been visualized in association with the cell surface via invaginations of the plasma membrane by using immunoelectron microscopy (Mulholland *et al.*, 1994). The actin cytoskeleton plays an important role in secretion and endocytosis, in addition to its essential functions in maintenance of cell shape, bud formation, polarized growth, and organelle distribution (Novick and Botstein, 1985; Kübler and Riezman, 1993; Welch *et al.*, 1994). Many cytoskeleton proteins have been isolated and characterized by using genetic and biochemical methods (Welch *et al.*, 1994). Mutations in the genes encoding different cytoskeleton proteins affect a subset of actin-dependent processes (Adams and Pringle, 1984; Drubin, 1991). This suggests that the various functions of the cytoskeleton rely on a particular combination of actin, actin-bundling, actin-binding, and/or motor protein components.

Actin filaments were suggested to participate in directed secretion because temperature-sensitive *act1–1* and *act1–2* mutants exhibited a partial defect late in the secretory pathway (Golgi to the plasma membrane) with intracellular accumulation of invertase and secretory vesicles (Novick and Botstein, 1985). Furthermore, mutations in *SAC1*, identified by virtue of their capacity to suppress actin mutations (Novick

† Present address: European Molecular Biology Laboratory, Meyerhofstrasse 1, D-69117 Heidelberg, Germany.
‡ Both of these authors contributed equally to this work.
¶ Corresponding author: Institut de Biologie Moléculaire et Cellulaire-Centre National de la Recherche Scientifique, 15 rue Descartes, 67084 Strasbourg, France.

et al., 1989), were also capable of rescuing *sec* mutations, which are impaired in transport beyond the Golgi (Cleves *et al.*, 1989). Disruption of the yeast tropomyosin gene *TPM1* results in both the apparent loss of actin cables and accumulation of secretory vesicles. Cell surface delivery of a-agglutinin also appears to be affected in this disruptant, but no defect was observed in secretion of invertase (Liu and Bretscher, 1992). A similar phenotype was observed for a temperature-sensitive *myo2–66* mutant, defective in a class V myosin. These mutant cells show mislocalization of actin and accumulate vesicles selectively in the mother cells, although the transit times of several secreted proteins are normal (Johnston *et al.*, 1991). Thus, alterations in the distribution of the actin cytoskeleton have various effects on post-Golgi traffic, which has recently been shown to involve at least two parallel pathways (Harsay and Bretscher, 1995).

Mutants in the cytoskeletal components, actin, and fimbrin (actin-bundling protein encoded by *SAC6*) were shown to be defective in the internalization step of receptor mediated endocytosis (Kübler and Riezman, 1993). On the other hand, *end3–1* and *end4–1*, which were identified as deficient in the first step of endocytosis, also show actin delocalization (Raths *et al.*, 1993; Bénédetti *et al.*, 1994). Sequencing of the *END4* gene revealed that it was identical to *SLA2*, deletion of which is synthetically lethal with deletion of the gene encoding the actin-binding protein Abp1p (Holtzman *et al.*, 1993). Both *sla2Δ/end4Δ* and *abp1Δ* are also synthetically lethal with a number of mutant actin alleles (Holtzman *et al.*, 1994). Three other *END* genes, *END5*, *END6*, and *END7* (Munn *et al.*, 1995) are allelic to *VRP1/MDP2*, *RVS161*, and *ACT1*, respectively, all previously shown to be required for normal distribution of cortical actin patches (Novick and Botstein, 1985; Donnelly *et al.*, 1993; Sivadon *et al.*, 1995). Similarly, type I myosins (Myo3p and Myo5p) were shown to be required for actin cytoskeleton organization and for fluid-phase and receptor-mediated endocytosis (Geli and Riezman, 1996; Goodson *et al.*, 1996). Finally, a recent screen for endocytic mutants based on sorting cells defective for internalization of the lipophilic dye FM 4–64 [*N*-(3-triethylammoniumpropyl)-4-(*p*-diethylaminophenylhexatrienyl)pyridinium dibromide] led to the identification of *DIM1* and *DIM2* genes (Wendland *et al.*, 1996), respectively allelic to *SHE4* (Jansen *et al.*, 1996) and *PAN1* (Sachs and Deardoff, 1992, 1995; Tang and Cai, 1996), both of which are also required for normal distribution of the actin cytoskeleton. Thus, a number of mutant proteins that alter cortical actin distribution cause a block in the internalization step of endocytosis and vice versa. This might be an indication that a functional actin cytoskeleton is required for the internalization step of endocytosis. However, mutation or deletion of several genes encoding actin-binding proteins that cause altered actin patch distribution, including *myo2–66*, *tpm1Δ*, *abp1Δ*, and *pfy1Δ* (profilin), do not appear to affect endocytosis (Kübler and Riezman, 1993; Kübler *et al.*, 1994; Munn *et al.*, 1995; Geli and Riezman, 1996). It has been suggested that endocytosis might be dependent on cortical patch structure but not on their cell cycle-dependent localization (Munn *et al.*, 1995).

Arp2p, a member of the large family of actin-related proteins, is an essential protein first identified in *S. cerevisiae* (Schwob and Martin, 1992). Using peptide-specific antibodies, it has recently been localized in cortical patches and is concentrated in areas of cell surface growth throughout the cell cycle, a localization overlapping that of actin cortical patches (Moreau *et al.*, 1996). This is consistent with results in *Acanthamoeba* where Arp2p has been isolated as a component of a seven-member complex of polypeptides (Machesky *et al.*, 1994) and is concentrated in the actin-rich cortex (Kelleher *et al.*, 1995). The thermosensitive *S. cerevisiae* mutant *arp2–1* (previously referred to as *arp2-H330L*; Moreau *et al.*, 1996) displays mild osmosensitivity, altered polarity of budding in diploid cells, and a disorganized actin cytoskeleton after extended time at a nonpermissive temperature, a phenotype typical of cytoskeletal mutants. Mutant *arp2–1* cells also showed reduced labeling with Lucifer yellow (LY), a fluid phase endocytosis marker, suggesting they might be defective in endocytosis (Moreau *et al.*, 1996). In the present report, we have used the *arp2–1* mutant to determine whether and how Arp2p participates in secretion and endocytosis.

A number of markers have been used to assess the status of the secretory pathway in yeast. These include periplasmic glycoproteins such as invertase (Schekman and Novick, 1982), proteins secreted into the extracellular medium such as the pheromone α-factor (Julius *et al.*, 1984; Nelson *et al.*, 1996), and plasma membrane permeases (Novick and Schekman, 1979; Tschopp *et al.*, 1984) including uracil permease, which we use in this study. Uracil permease, encoded by the *FUR4* gene (Jund *et al.*, 1988), is targeted to the plasma membrane where it undergoes phosphorylation on multiple serine residues (Volland *et al.*, 1992). We have examined the role of Arp2p in the secretory pathway by using invertase and the uracil permease as reporter proteins. In addition, mutant cells were examined by thin-section electron microscopy (EM) to detect possible accumulation of vesicles.

Several reporter systems have recently been developed to follow endocytosis in yeast. The dye LY is commonly used to follow fluid phase endocytosis (Riezman, 1993), and the vital stain FM 4–64 is used to follow bulk membrane internalization and transport to the vacuole (Vida and Emr, 1995). The α-factor pheromone has been largely used to follow receptor-mediated (Ste2p) endocytosis (Singer and Riezman, 1990; Riezman, 1993). Direct assessment of a-factor

Table 1. Yeast strains

Strains	Genotype	Source
NY13	*MATa, gal2, ura3-52*	P. Novick
NY17	*MATa, gal2, ura3-52, sec6*	P. Novick
NY279	*MATa, act1-3, gal2, ura3-52*	P. Novick
RH144-3D	*MATa, his4, ura3, leu2, bar1-1*	H. Riezman
RH266-1D	*MATa, his4, ura3, leu2, bar1-1, end3-1*	H. Reizman
RH268-1C	*MATa, his4, ura3, leu2, bar1-1, end4-1*	H. Riezman
YPH499	*MATa, ade2-101, his3-Δ200, leu2-Δ1, lys2-801, trp1-Δ63, ura3-52*	P. Hieter
YPH500	*MATα, ade2-101, his3-Δ200, leu2-Δ1, lys2-801, trp1-Δ63, ura3-52*	P. Hieter
YMW82	*MATα, arp2-1, ade2-101, his3-Δ200, leu2-Δ1, lys2-801, trp1-Δ63, ura3-52*	Moreau *et al.*[a] (1996)
JHRY60-4A	*MATa, his4-519, ura3-52, leu2-3, -112, lys2 vpl2-2*	T. Stevens
JHRY28-3B	*MATa, ade6, his-519, leu2-3, -112, lys2*	T. Stevens
SEY5016	*MATα, sec1-1, ura3-52, leu2-3, -112, SUC2*	R. Schekman

[a] *arp2-1* is the allele number for *arp2-H330L*.

receptor (Ste3p) internalization was also reported (Davis *et al.*, 1993). Another sensitive way to follow endocytosis is to measure clearance of permease transporters from the plasma membrane and their subsequent vacuolar degradation (Volland *et al.*, 1994; Lai *et al.*, 1995; Riballo *et al.*, 1995). Similar mechanisms underlie receptor-mediated endocytosis and endocytosis of several transporters. Internalization was reported to be *END3* and *END4* dependent in the cases studied so far (Raths *et al.*, 1993; Kölling and Hollenberg, 1994; Lai *et al.*, 1995; Riballo *et al.*, 1995; Volland *et al.*, 1994; Egner and Kuchler, 1996). Furthermore, internalization of uracil permease was shown to be *ACT1* dependent (Galan *et al.*, 1996). It was recently demonstrated that an ubiquitination step is required before internalization of Ste2p and Ste3p receptors (Hicke and Riezman, 1996; Roth and Davis, 1996), ABC transporters (Kölling and Hollenberg, 1994; Egner and Kuchler, 1996), and uracil permease (Galan *et al.*, 1996). Ubiquitinated forms of these proteins accumulate in mutants impaired in the internalization step of endocytosis. Here, we analyze the internalization step of endocytosis by following the fate of the plasma membrane uracil permease and its ubiquitinated forms. The integrity of later steps of the endocytic pathway was tested by following biosynthetic delivery and processing of the soluble vacuolar hydrolase carboxypeptidase Y (CPY).

MATERIALS AND METHODS

Strains, Plasmids, and Growth Conditions

Strains used in this study are listed in Table 1. Because the chromosome-encoded uracil permease is produced in very low concentration, cells that expressed permease from multicopy plasmids were used for the immunodetection of the protein. The multicopy plasmid p195 gF (2μ *URA3 GAL-FUR4*; Volland *et al.*, 1994) carries the *FUR4* gene (Jund *et al.*, 1988) under the control of the *GAL10* promoter. Plasmid YEp96 (Ecker *et al.*, 1987) contains a synthetic yeast ubiquitin gene under control of the copper-inducible *CUP1* promoter. YEp112 is identical to YEp96, except that it encodes an hemagglutinin-tagged version of ubiquitin (Hochstrasser *et al.*, 1991). Yeast strains were transformed as described by Gietz *et al.* (1992). Cells were grown at 30°C (or 24°C for thermosensitive strains) in rich medium (YP) or minimal medium (YNB) containing 0.67% yeast nitrogen base without amino acids (Difco, Detroit, MI) supplemented with appropriate nutrients. Carbon source was 2% glucose or 4% galactose plus 0.05% glucose. Overexpression of the *CUP1* promoter was induced with 0.1 mM $CuSO_4$.

Invertase Assay

Cells were grown at 24°C in YP medium containing 2% glucose to 5×10^6 cells/ml. After preincubation for 15 min at 37°C, cells were washed with prewarmed water, resuspended in YP medium containing 0.1% glucose, and incubated at 37°C. Invertase assays were performed as described by Goldstein and Lampen (1975) using incubations without sucrose as control. At each time point, 2×10^7 cells were pelleted, washed, and resuspended in 500 μl of 10 mM NaN_3. Half of the sample was used to assay the amount of external invertase and the other half was used to assay internal invertase. External invertase levels were measured on intact cells and internal invertase levels were measured in spheroplast lysates as described by Novick and Botstein (1985). The percentage of secreted invertase corresponds to external invertase divided by total invertase (external plus internal).

Measurement of Uracil Uptake

Uracil uptake was measured in exponentially growing cells as previously described (Volland *et al.*, 1992). One milliliter of yeast culture was incubated with 5 μM [^{14}C]uracil (Amersham, France) for 20 s at 30°C and then quickly filtered through Whatman GF/C filters, which were washed twice with ice-cold water, and radioactivity was measured.

EM

Cultures of *arp2–1* and *act1-3* mutant cells and their corresponding wild-type strains were grown to exponential phase in rich medium at 24°C. Half of each culture was transferred to 37°C; the *arp2–1* mutant and its parent were incubated for 2 h, and the *act1-3* mutant and its parent were incubated for 1 h. Cells were fixed with 2.5% glutaraldehyde in cacodylate buffer (0.1 M, pH 7.2) for 1 h at room temperature then washed and postfixed in 1% osmium tetroxide in the same buffer. Fixed cells were dehydrated in a graded ethanol series and embedded in Epon-araldite resin. Ultrathin sections were

stained for 3 min with ruthenium red (1‰ in water; a powerful stain for polysaccharides; Muftaschiev, personal communication), poststained with uranyl acetate (0.5% in water) for 1 min, and examined in a Philips EM410 electron microscope. Vesicles were counted in 30–50 well-stained cells cut along the mother-bud axis.

Yeast Cell Extracts and Western Immunoblotting

Cell extracts were prepared and proteins were analyzed by immunoblots as described previously with an antiserum to the last 10 residues of uracil permease (Volland *et al.*, 1994). Some immunoblots were also probed with an antiserum to plasma membrane [H^+]ATPase. Primary antibodies were detected with a horseradish peroxidase-conjugated anti-rabbit IgG secondary antibody followed by ECL chemiluminescence (Amersham).

Membrane Preparation

Yeast cells (80 A_{600}) in exponential growth phase were harvested by centrifugation in the presence of 10 mM sodium azide and used to prepare plasma membrane-enriched fractions as described previously (Galan *et al.*, 1996). Membrane-bound proteins were examined by Western blot analysis as described above.

Pulse-Chase Labeling and Immunoprecipitation of CPY

Cells were grown in YNB medium with glucose as a carbon source to an A_{600} of 1.0 (2×10^7 cells/ml). They were collected, resuspended in fresh medium at an A_{600} of 10, and preincubated for 15 min at 37°C. Cells were labeled for 5 min by adding [^{35}S]methionine at 150 μCi/ml of culture and chased with 10 mM unlabeled methionine. Aliquots of the culture (0.3 ml) were removed at various times during the chase, and cell extracts were prepared by lysis with 0.2 M NaOH for 10 min on ice. Trichloroacetic acid was added to a final concentration of 5%, and the samples were incubated for an additional 10 min on ice. Proteins were processed for immunoprecipitation as described previously (Volland *et al.*, 1992), except that they were heated for 4 min at 95°C. Immunoprecipitated proteins were separated by SDS-PAGE on 7.5% gels and treated by fluorography as previously described (Volland *et al.*, 1992).

FM 4–64 Staining

Staining with the fluorescent dye FM 4–64 was done as described by Vida and Emr (1995). Strains were grown in YP medium at 25°C to an A_{600} of 0.8. After preincubation for 15 min at 25°C or 37°C, cells were harvested and resuspended in fresh medium at 20–40 A_{600}. FM 4–64 (Molecular Probes, Eugene, OR) was added to 16 μM from a stock solution of 1.6 mM in dimethyl sulfoxide, and cells were incubated with shaking for 15 min at 25°C or 37°C. The cells were harvested, resuspended in fresh YP medium at 10–20 A_{600}, and incubated with shaking for 30 or 60 min at 25°C or 37°C. After this chase step, cells were collected, resuspended two or three times more concentrated in fresh YP, and then mounted on slides. Fluorescence was visualized by using a XF39 filter on a Nikon Optiphot-2 microscope equipped with differential interference contrast optics.

RESULTS

arp2–1 Mutant Cells Are Not Defective in Cell Surface Delivery of Invertase and Uracil Permease

Yeast cell surface growth is dependent upon constitutive secretion culminating in the fusion of secretory vesicles with the bud membrane (Field and Schekman, 1980) in a process thought to involve the actin cytoskeleton (Novick and Botstein, 1985). The integrity of the secretory pathway was first assessed by examining export of the periplasmic enzyme invertase. Invertase is the product of the *SUC2* gene, which encodes two transcripts, one constitutive and the other glucose repressed (Carlson and Botstein, 1982). The product of the first transcript remains soluble in the cytoplasm. The product of the second transcript is targeted to the endoplasmic reticulum (ER) and is processed through the ER, where it becomes core-glycosylated. It is fully glycosylated in the Golgi apparatus and is then packaged into vesicles. The enclosed invertase is released into the periplasmic space, where its activity can be monitored on intact cells by using substrates unable to cross the plasma membrane. To detect possible defects in invertase export, invertase activity was compared in wild-type and *arp2–1* cells. As a control, *sec6* mutant cells, in which the last step of the secretory pathway is tightly blocked at the restrictive temperature (Novick *et al.*, 1980), were used. Exponentially growing cells in repressing medium were preshifted for 10 min to 37°C and resuspended in derepressing medium at 37°C. External and internal invertases were assayed at regular time intervals, and the results were expressed as percentage of secreted invertase (Figure 1). Periplasmic enzyme activity was measurable in wild-type cells 15 min after the onset of derepression. No remarkable difference in the kinetics of appearance of cell surface invertase activity was observed between *arp2–1* and wild-type cells (Figure 1A). This contrasts with *sec6* mutant cells (Figure 1B) where the secretion of invertase was grossly altered; newly synthesized active invertase accumulated almost entirely as an intracellular form. Furthermore, in *arp2–1* cells the internal invertase pool was not larger than in wild-type cells after 1 h of derepression at the restrictive temperature (our unpublished observations). Therefore, the rate of invertase secretion remains normal in the *arp2–1* mutant.

It is possible that *arp2–1* mutant cells may have a minor secretion defect not easily detectable by measurement of invertase activity. For this reason we also followed the intracellular fate of another marker of the secretory pathway, uracil permease (Volland *et al.*, 1992). Delivery of uracil permease to the cell surface can be monitored by measuring the increase in uracil permease activity that becomes detectable at the cell surface shortly after induction of its synthesis. To do this, wild-type and mutant cells were transformed with a multicopy plasmid encoding the *FUR4* gene under the control of the *GAL10* promoter. After exponential growth at 24°C, cells were submitted (or not) to a 15-min incubation at 37°C. Permease synthesis from the *FUR4* gene under the control of the *GAL10* promoter was then induced by the addition of galactose. Wild-type and *arp2–1* mutant cells showed similar

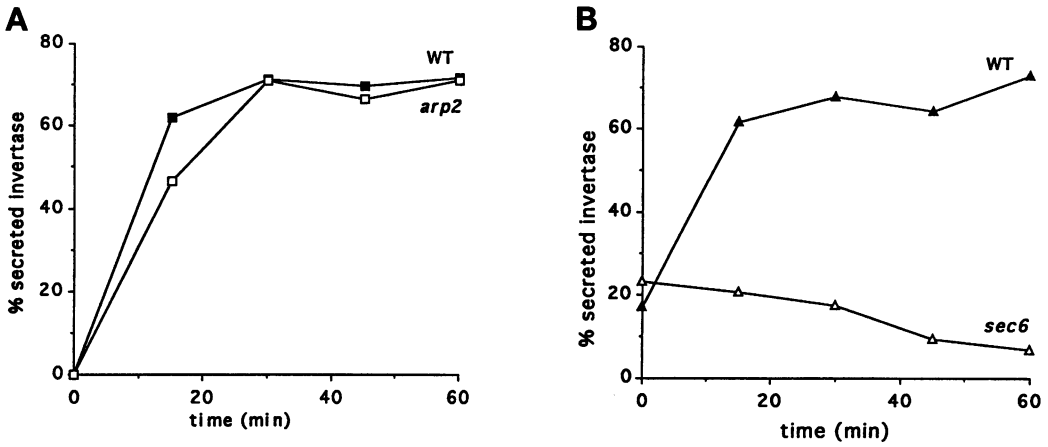

Figure 1. Invertase secretion is normal in *arp2–1* mutant cells. Cells were grown overnight in YPD medium. After a 15-min shift to 37°C, cells were pelleted and resuspended in YP medium containing 0.1% glucose and incubated at 37°C. At various time points, aliquots were removed and assayed for external and internal invertase. Results are plotted as a percentage of secreted/total (internal +external) invertase. (A) YMW81 (*arp2–1*) and YPH499 (WT). (B) NY17 (*sec6*) and NY13 (WT).

increase with time of induced permease activity during 2 h at both permissive and restrictive temperatures (Figure 2, A and B). In addition, no delay in permease phosphorylation was observed in pulse-chase experiments carried out in parallel at restrictive temperature with wild-type and *arp2–1* mutant cells (our unpublished observations). These experiments did not reveal any alteration in the plasma membrane delivery of uracil permease in the *arp2–1* mutant. In a parallel control experiment, uracil uptake was measured in *act1–3* (= *act1–1*) and parental wild-type cells, which showed a similar increase of uracil uptake at a permissive temperature (Figure 2C). At the restrictive temperature, the *act1–3* mutation prevented the increase of uracil uptake for more than 2 h (Figure 2D), whereas the level of immunodetectable permease increased similarly in wild-type and mutant cells (our unpublished results). Thus, the normal cell surface delivery of the permease protein in the *arp2–1* cells is in contrast with the severe defect caused by the *act1–3* mutation.

arp2–1 Mutant Cells Show a Limited Accumulation of Vesicles

Mutants in several cytoskeleton elements accumulate vesicles without showing other defects in secretion of known markers of the secretory pathway (Govindan *et al.*, 1995), whereas wild-type yeast cells contain only a few secretory vesicles (Schekman and Novick, 1982). We examined *arp2–1* mutant cells for ultrastructural and membrane vesicle defects and used *act1–3* cells, which are known to accumulate secretory vesicles at restrictive temperature (Novick and Botstein, 1985), as an affected control. Cells were grown at 24°C and then shifted to 37°C for 2 h. Ultrastructural examination first revealed that both *act1-3* and *arp2–1* mutant cells were somewhat larger than parental wild-type cells (Figure 3, compare a, b, and d) as described for *act1–1/act1–3* cells. In wild-type cells, we observed only a few vesicles, mostly located in the bud (Figure 3a). In contrast, the morphology of *act1-3* mutant cells was clearly altered; after 1 h at 37°C, a massive accumulation of vesicles and some lamellar structures were observed (Figure 3b). Even when grown at permissive temperature *act1-3*, cells showed some accumulation of vesicles. The situation observed in *arp2–1* mutant cells was quite distinct from that in *act1-3* cells. When the *arp2–1* mutant was grown at permissive temperature, cells were indistinguishable from wild-type. However, in *arp2–1* mutant cells after a 2-h incubation at the restrictive temperature, morphological changes were observed. Occasional lamellar structures (Figure 3, c and d, thin arrows) similar to structures that were frequently observed in *act1–3* mutant cells (Novick and Botstein, 1985; Goodson *et al.*, 1996) and membranous vesicles (Figure 3,c and d) were visible.

To better represent the image seen across the cell populations, the number of vesicles in budded cells was counted in 30–50 wild-type, *arp2–1*, and *act1-3* mutant cells. Results showing the distribution of the number of membranous vesicles per cell for each strain are represented in histograms in Figure 4. About 50% of *arp2–1* mutant cells showed no major changes, 40% showed minor changes, and <10% (see examples in Figure 3, c and d) accumulated a large (>20) number of vesicles. At 37°C, fewer vesicles accumulated in *arp2–1* cells compared with *act1–3* cells although there was a slight accumulation in *arp2–1* compared with wild-type cells. In summary, from the results shown in Figures 2–4, we conclude that although a severe defect in plasma membrane delivery of uracil permease in *act1–3* cells can be correlated with a dramatic increase in the number of accumulated vesicles, the limited accumulation of vesicles observed in *arp2–1* mutant cells after 2 h at restrictive

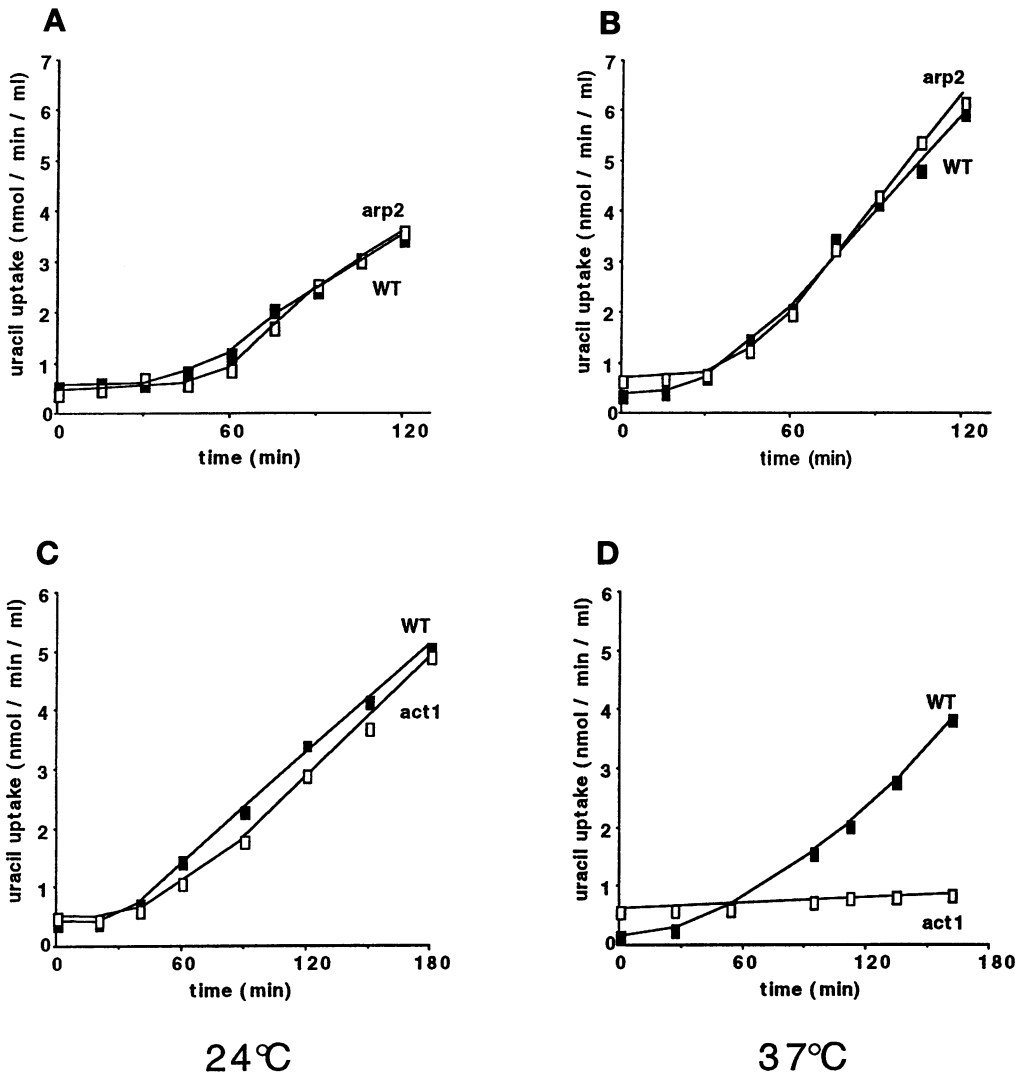

Figure 2. Cell surface delivery of uracil permease is normal in *arp2–1* mutant cells and defective in *act1–3* mutant cells. (A and B) YPH500 (WT) and YMW82 (*arp2–1*) mutant cells were transformed with p195gF (2μ *GAL-FUR4*). Cells were grown at permissive temperature with lactate (2%) as a carbon source to an A_{600} of 0.5. Galactose was added to the medium at 24°C (A) or after a 15-min shift to 37°C (B), and permease induction was followed by measuring uracil uptake activity at various times thereafter. We observed similar results with cells grown in raffinose as a carbon source before galactose induction. The same experiment was performed at 24°C (C) or 37°C (D) on NY13 (WT) and NY279 (*act1–3*) cells grown in raffinose. No induction was observed in *act1–3* cells grown in lactate. Chromosomal-encoded permease levels are very low.

temperature is not associated with an alteration in cell surface delivery of invertase or uracil permease.

The arp2–1 Mutant Is Defective in the Internalization Step of Endocytosis

Previous observations suggested that Arp2p could be involved in the endocytic pathway. The *arp2–1* mutant was deficient in the uptake of LY, a lipophilic dye that accumulates in the vacuole (Moreau *et al.*, 1996). This might indicate defective internalization or, alternatively, defective vacuolar targeting. The small amount of LY that entered the cells appeared to stain the vacuole. This suggested that internalization of LY rather than its transport to the vacuole was altered. To expand upon these preliminary results, we investigated the effect of the *arp2–1* mutation on the internalization step of endocytosis by measuring the clearance of uracil permease from the plasma membrane. Uracil permease was previously shown to undergo basal endocytosis and degradation in actively growing cells (Galan *et al.*, 1996). Stress conditions, such as heat shock, nutrient deprivation, or inhibition of protein synthesis, result in an acceleration of the permease turnover rate (Volland *et al.*, 1994). Both basal and induced turnover depend on the Npi1p/Rsp5 ubiquitin ligase (Hein *et al.*, 1995; Galan *et al.*, 1996), required for permease ubiquitination (Galan *et al.*, 1996). Once internalized, permease is degraded in the vacuole in a *PEP4*-dependent but proteasome-independent way (Galan *et al.*, 1996).

The fate of plasma membrane uracil permease was followed at permissive and restrictive temperatures in wild-type and *arp2–1* cells expressing uracil permease under the control of the *GAL10* promoter,

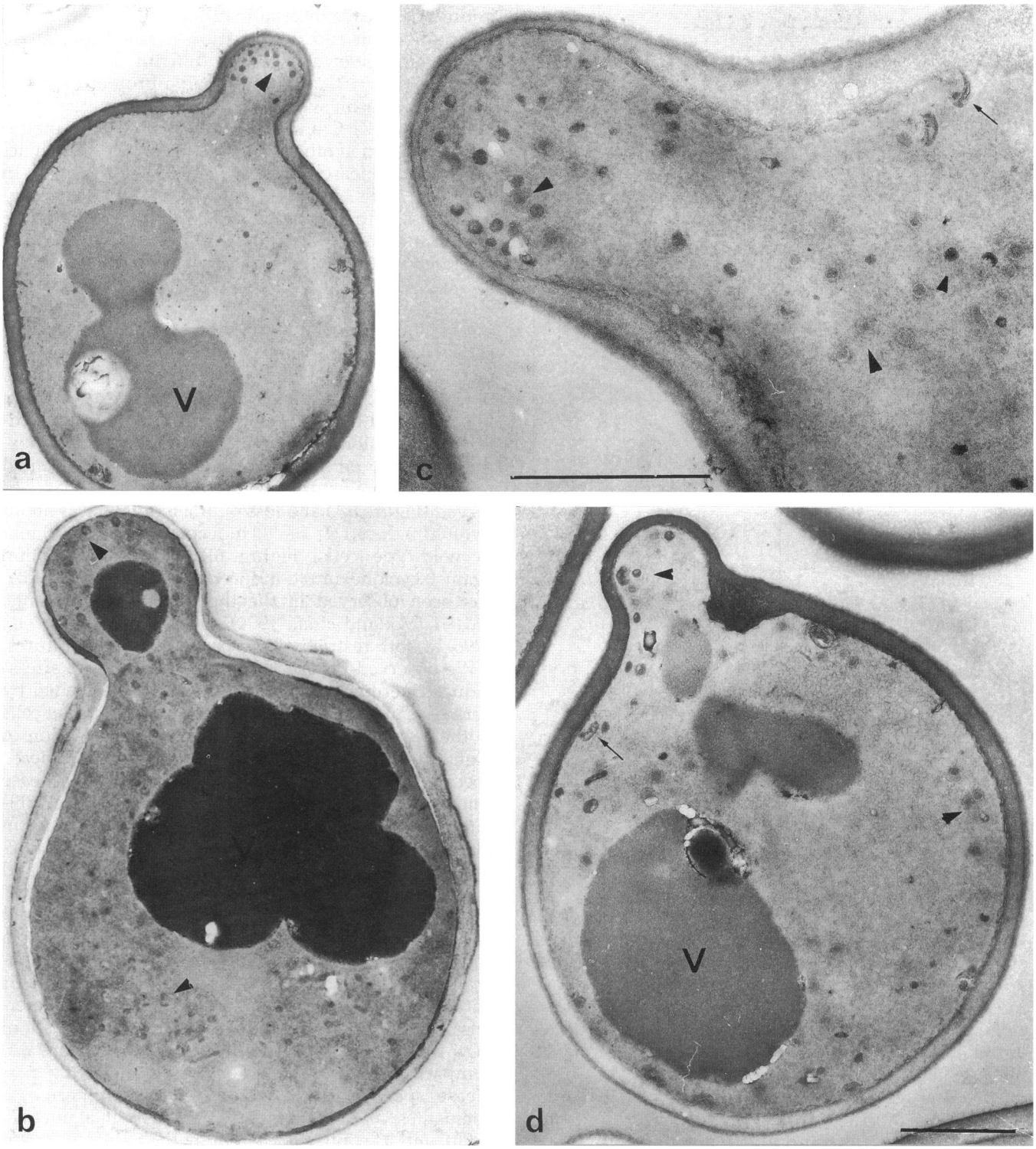

Figure 3. Electron micrographs of thin sections of wild-type (YPH500) (a), *act1–3* mutant (NY279) cells (b), and *arp2–1* mutant (YMW82) cells (c and d) after incubation at restrictive temperature. Cells were grown at 24°C in YPD medium. Aliquots withdrawn before or after transfer to 37°C were fixed and processed for EM as described in MATERIALS AND METHODS. Representative images of cells withdrawn after 2 h (a, c, and d) or 1 h (b) at 37°C are shown. *act1–3* cells were left for only 1 h at 37°C because many *act1–3* cells exhibited dramatic overall structural damage after 2 h at 37°C (our EM observation), in agreement with the observation that *act1–3* cells begin to die before 2 h at 37°C (Novick and Botstein, 1985). Arrowheads, small vesicles; thin arrows, lamellar structures. Bar, 1 μm.

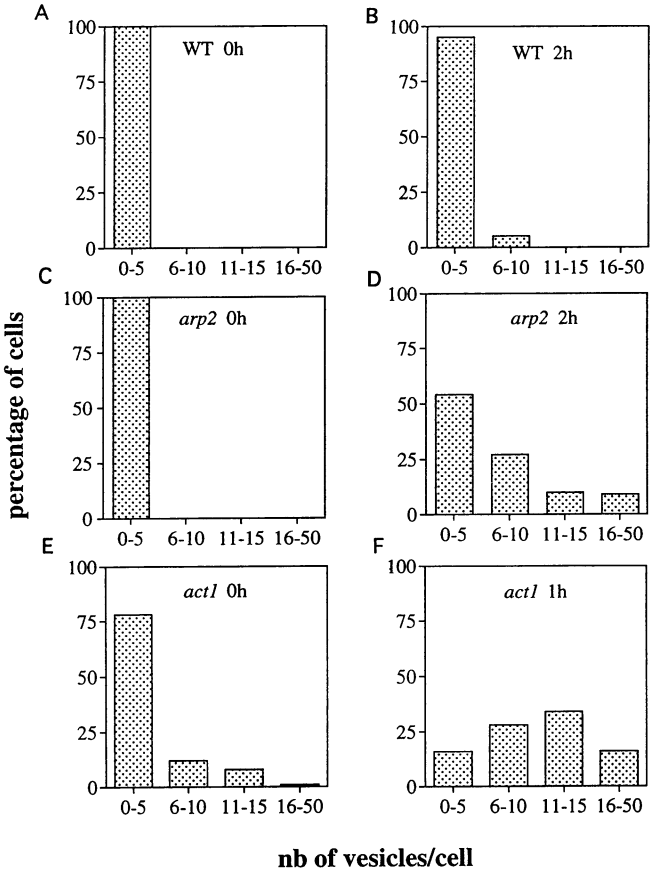

Figure 4. Accumulation of vesicles in *arp2–1* cells at 37°C. Experimental conditions are described in Figure 3. Vesicles were counted only in well-stained cells cut along the bud-mother axis in 30 cells for *act1–3* or in 50 cells for wild-type and *arp2–1* cells, which contained fewer vesicles. Results are given as the number (nb) of vesicles per cell.

after repression by glucose of new permease synthesis. Uracil uptake was measured and protein extracts were prepared and analyzed for uracil permease by Western immunoblotting (Figure 5). Exponentially growing wild-type and mutant cells showed the same pattern of steady-state permease species, with electrophoretic mobilities corresponding to different phosphorylation states. In wild-type cells, a heat shock from 24°C to 37°C greatly accelerated the loss of uracil uptake ($t_{1/2}$ = 300 and 40 min, respectively, Figure 5B). At both temperatures, permease degradation (Figure 5A) appeared to parallel the loss of uracil uptake (Figure 5B), suggesting that the temperature shift affected primarily the rate of permease internalization. At the restrictive temperature, the *arp2–1* mutation provided strong protection against permease degradation and about fivefold protection against the loss of uracil uptake ($t_{1/2}$ = 240 min, compared with 40 min in wild-type cells, Figure 5B), indicating that the mutation prevented permease internalization. At 24°C, however, internalization and degradation of uracil permease are much slower and it was difficult to determine whether the *arp2–1* mutation had a protective effect.

For this reason we also examined permease internalization at 24°C and 37°C after a stress, the inhibition of protein synthesis by cycloheximide, which accelerates permease turnover (Volland *et al.*, 1994). In wild-type cells, inhibition of protein synthesis triggered loss of uracil uptake and concomitant permease degradation at 24°C, both of which were further accelerated when the temperature was raised from 24°C to 37°C (Figure 6). At the restrictive temperature, the *arp2–1* mutation provided strong protection against degradation of uracil permease and loss of uracil uptake ($t_{1/2}$ = 140 min, compared with 20 min in wild-type cells). This effect is similar to that seen in the preceding experiment where permease expression was inhibited by repression of transcription. In addition, after inhibition of protein synthesis by cycloheximide at the permissive temperature, a substantial protection against permease degradation was observed (Figure 6A) and loss of uracil uptake was about twofold reduced ($t_{1/2}$ = 80 min compared with 40 min in wild-type cells, Figure 6B). Similar protection against cycloheximide-induced loss of uracil uptake has been observed in the thermosensitive mutants, *end4–1* (Volland *et al.*, 1994) and *act1-3* (Galan *et al.*, 1996) at both restrictive and permissive temperatures.

We observed previously that both basal and stress-induced permease internalization were preceeded by permease ubiquitination. A shift of *arp2–1* mutant cells to the restrictive temperature results in formation of high molecular weight regularly spaced permease species that likely correspond to ubiquitin-permease conjugates (Figures 5A and 6A, first lanes). Since ubiquitinated forms of uracil permease are seen better in plasma membrane-enriched preparations, these fractions were prepared from growing wild-type and *arp2–1* mutant cells shifted or not for 10 min to 37°C (Figure 7A). Whereas wild-type and *arp2–1* mutant cells contained the same amount and pattern of a control protein, the stable and abundant plasma membrane [H^+]ATPase, they differed considerably in their pattern of permease species. When grown at the permissive temperature, *arp2–1* cells were enriched in high molecular weight permease species (Figure 7A, compare lanes 1 and 2). These slow-migrating permease species corresponded to ubiquitin-permease conjugates, as demonstrated previously (Galan *et al.*, 1996), and as confirmed herein by their shift to higher molecular weight upon overexpression of an epitope-tagged version of ubiquitin (Figure 7B). Incubation with cycloheximide for 10 min at 37°C led to a further enrichment of these conjugates in *arp2–1* cells (Figure 7A, lane 4). This spectacular accumulation of ubiquitin-permease conjugates in *arp2–1* cells at both per-

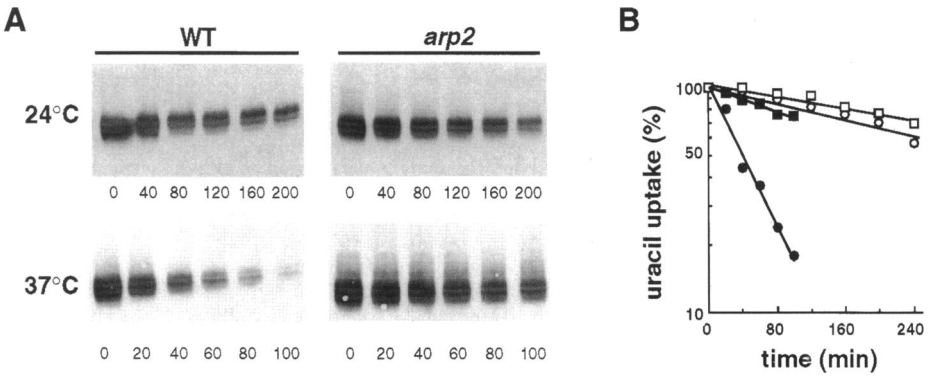

Figure 5. Defective internalization of uracil permease after repression of the transcription of the *FUR4* gene at restrictive temperature in *arp2–1* cells. YPH500 (WT) and YMW82 (*arp2–1*) strains transformed with the plasmid p195gF (2μ *URA3 FUR4*) were grown at 24°C to an A_{600} of 0.6 with galactose as carbon source. Cells were transferred or not to 37°C for 10 min and glucose was added to 2% to repress permease synthesis. (A) Protein extracts from WT and *arp2–1* cells were prepared at the times indicated after the addition of glucose. Aliquots corresponding to 0.2 ml of growing cultures were analyzed for uracil permease by immunoblotting. (B) Uracil uptake (permease activity) was measured at different times after the addition of glucose. Results are expressed as a percentage of initial activities. ○, WT 24°C; ●, WT 37°C; □, *arp2–1* 24°C; ■, *arp2–1* 37°C.

missive and restrictive temperatures confirmed the involvement of Arp2p in the internalization step of endocytosis.

Vacuolar Delivery of Soluble Hydrolases Is Normal in arp2–1 Mutant Cells

The lack of degradation of uracil permease in *arp2–1* mutant cells could result from defects in vacuolar delivery, in addition to defects in the internalization step of endocytosis. The yeast vacuole receives material from two vesicular pathways, biosynthetic vesicular traffic from the Golgi apparatus and endocytic vesicular traffic from the cell surface. Evidence has been presented to show that these two pathways converge at a prevacuolar endosomal compartment (late endosome; Vida *et al.*, 1993). We checked whether biosynthetic delivery and processing of vacuolar hydrolases is affected in *arp2–1* mutant cells, by using CPY as a marker. CPY is synthesized as a precursor that is translocated into the lumen of the ER where it is core glycosylated. This ER form of CPY (p_1CPY) is 67 kDa. In the medial Golgi compartment, CPY is further glycosylated, which increases its size to 69 kDa (p_2CPY). CPY is finally transported via late endosomes to the vacuole, where it is matured by proteinase A to the 61-kDa mature species (mCPY; Graham and Emr, 1991). The intracellular fate of CPY was analyzed by a pulse-chase experiment at restrictive

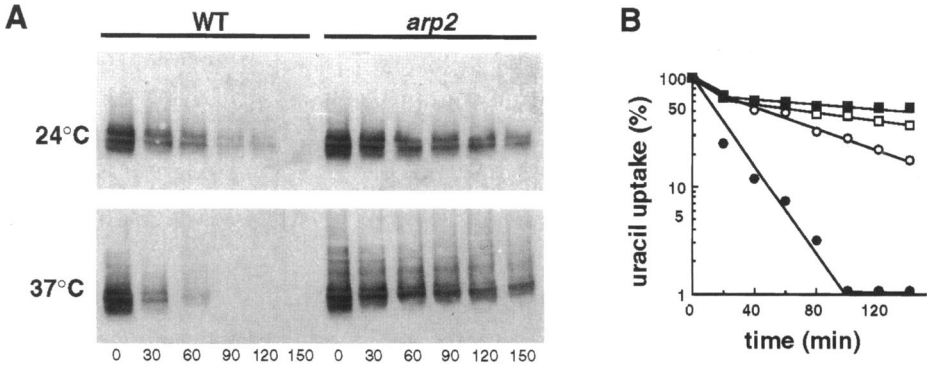

Figure 6. Defective internalization of uracil permease in *arp2–1* cells after inhibition of protein synthesis. YPH500 (WT) and YMW82 (*arp2*) strains transformed with the plasmid p195gF (2μ *URA3 GAL-FUR4*) were grown at 24°C to an A_{600} of 0.6 with galactose as carbon source. Cells were transferred or not for 10 min to 37°C, and cycloheximide was added to a final concentration of 100 μg/ml. (A) Protein extracts from WT and *arp2–1* cells were prepared at the times indicated after the addition of cycloheximide. Aliquots corresponding to 0.2 ml of culture were analyzed for uracil permease protein by Western immunoblotting. (B) Uracil permease activity (uptake) was measured at different times after the addition of cycloheximide. Results are expressed as a percentage of the initial activities. ○, WT 25°C; ●, WT 37°C; □, *arp2–1* 25°C; ■, *arp2–1* 37°C.

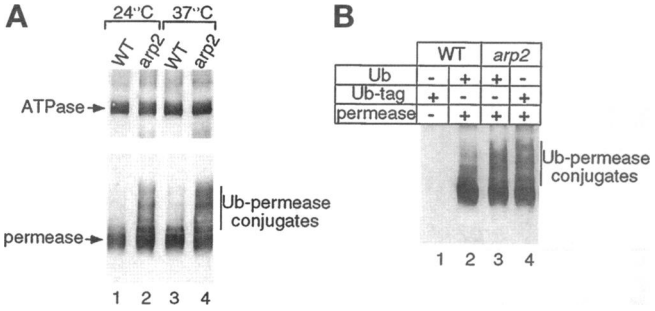

Figure 7. Ubiquitin (Ub)-permease conjugates accumulate in *arp2–1* cells. (A) YPH500 (WT) and YMW82 (*arp2–1*) cells transformed and grown as described in Figure 5 were collected before (lanes 1 and 2) or after (lanes 3 and 4) incubation for 10 min at 37°C with cycloheximide. They were used to prepare plasma membrane-enriched fractions. Aliquots containing the same amount of proteins were separated by SDS-PAGE and analyzed by immunoblotting for uracil permease and [H^+]ATPase proteins. Ub-permease conjugates are indicated by a vertical line. (B) Plasma membrane-enriched fractions were prepared from YPH500 cells (WT) transformed with plasmid YEp112 (Ub tag) alone (lane 1) or transformed with plasmid p195 gF (2μ *URA3 GAL-FUR4*) plus YEp96 (Ub; lane 2); membrane fractions were prepared from YMW82 (*arp2*) transformed with p195gF plus YEp96 (lane 3) or p195gF plus YEp112 (lane 4). Cells were grown in the presence of $CuSO_4$ (0.1 mM) to induce the expression of ubiquitin.

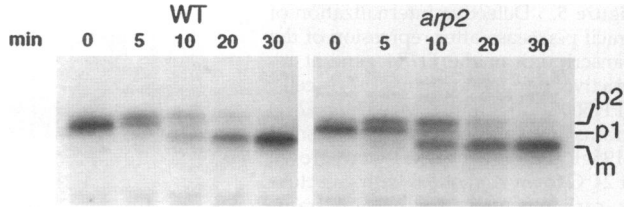

Figure 8. *arp2- 1* mutant shows wild-type maturation of the soluble vacuolar protein CPY. YPH500 (WT) and YMW82 (*arp2*) cells were pulse labeled with [S^{35}]methionine and chased with nonradioactive methionine as described in MATERIALS AND METHODS, until the indicated times. CPY was immunoprecipitated from samples taken at various time points. The immunoprecipitates were analyzed on 7.5% polyacrylamide-SDS gels and visualized by fluorography. p1, ER form; p2, Golgi form; m, mature vacuolar form.

temperature in wild-type and *arp2–1* mutant cells (Figure 8). Processing of CPY appeared as a rapid event in both wild-type and mutant cells; the p_2 form appeared after only a 5-min chase, and the protein was entirely matured within 20 min. Thus, CPY trafficking from the ER to the vacuole appears to be normal in *arp2–1* mutant cells.

Effect of the arp2–1 Mutation on FM 4–64 Transport

We used the lipophilic dye FM 4–64 as a reporter of vacuolar dynamics. FM 4–64 is a vital dye that has been recently proposed for tracing plasma membrane to vacuole transport via endosome intermediates (Vida and Emr, 1995). Growing cells were concentrated in fresh medium, dye was added to the extracellular medium for a short pulse, and then cells were washed and resuspended in medium without FM 4–64 to induce a chase. We followed FM 4–64 transport to the vacuole at 24°C and, as shown in Figure 9, at 37°C in wild-type and *arp2–1* cells, as well as in *sec1* and *vpl2* (a class E vacuolar sorting mutant) cells as impaired controls. After a 30-min chase at 37°C, normal dye labeling was seen in wild-type (Figure 9A, right) and *arp2–1* (Figure 9B, right) cells. A few discrete intracellular fluorescent dots, most likely endosomes, were detectable and some of the dye had already labeled the membrane of structures within the cell that correspond to the vacuole, visualized by differential interference contrast optics (Figure 9, A and B, left). Further incubation showed essentially vacuolar label in both wild-type and *arp2–1* cells. Hence, transport via endosomes to the vacuole did not appear affected in the *arp2–1* mutant strains even at the nonpermissive temperature. This contrasts with the situation observed in the control strains. At the nonpermissive temperature, even after a chase of 60 min, the *sec1* mutant cells localized the dye poorly (Figure 9C). FM 4–64 was observed as diffuse punctate staining in the cytoplasm, as had been reported previously (Vida and Emr, 1995). In the *vpl2* control strain (Figure 9D), dye had not reached the vacuolar membrane after a 60-min chase at 37°C but accumulated in organelles proximal to the vacuole (presumably late endosomes), whereas vacuolar labeling was evident in the wild-type parental cells (Figure 9E).

Although the rate of transit of the dye from the plasma membrane to the vacuolar membrane did not appear to be modified in the *arp2-1* strain relative to wild type, general staining was less intense in most *arp2-1* cells (Figure 9, compare A and B). Overall fluorescence of the population of stained cells appears to be reduced by the *arp2–1* mutation, although dye uptake was not strictly quantified. These findings are similar to the situation described for *end3–1* and *end4–1* mutations. Vida and Emr (1995) reported that FM 4–64 transit was normal in *end3–1* and *end4–1* cells. More recent results cited a reduction in FM 4–64 internalization in these mutants with an associated decrease (two- to fourfold) of fluorescent signal in the vacuolar membrane (Wendland *et al.*, 1996).

Figure 9 (facing page). Vacuolar membrane staining with the lipophilic dye FM 4–64. YPH500 (ARP2) (A), YMW82 (*arp2–1*) mutant cells (B), SEY5016 (*sec1*) mutant cells (C), JHRY60–4A(*vpl2*) mutant cells (D), and their parental cells JHRY28–3B (E) were grown in YPD at 25°C and shifted to 37°C for 15 min. FM 4–64 was added and cells were incubated for 15 min at 37°C. Cells were harvested by centrifugation, taken up in prewarmed YPD medium (to remove the free dye), and further incubated at 37°C for 30 min (A and B) or 60 min (C–E).

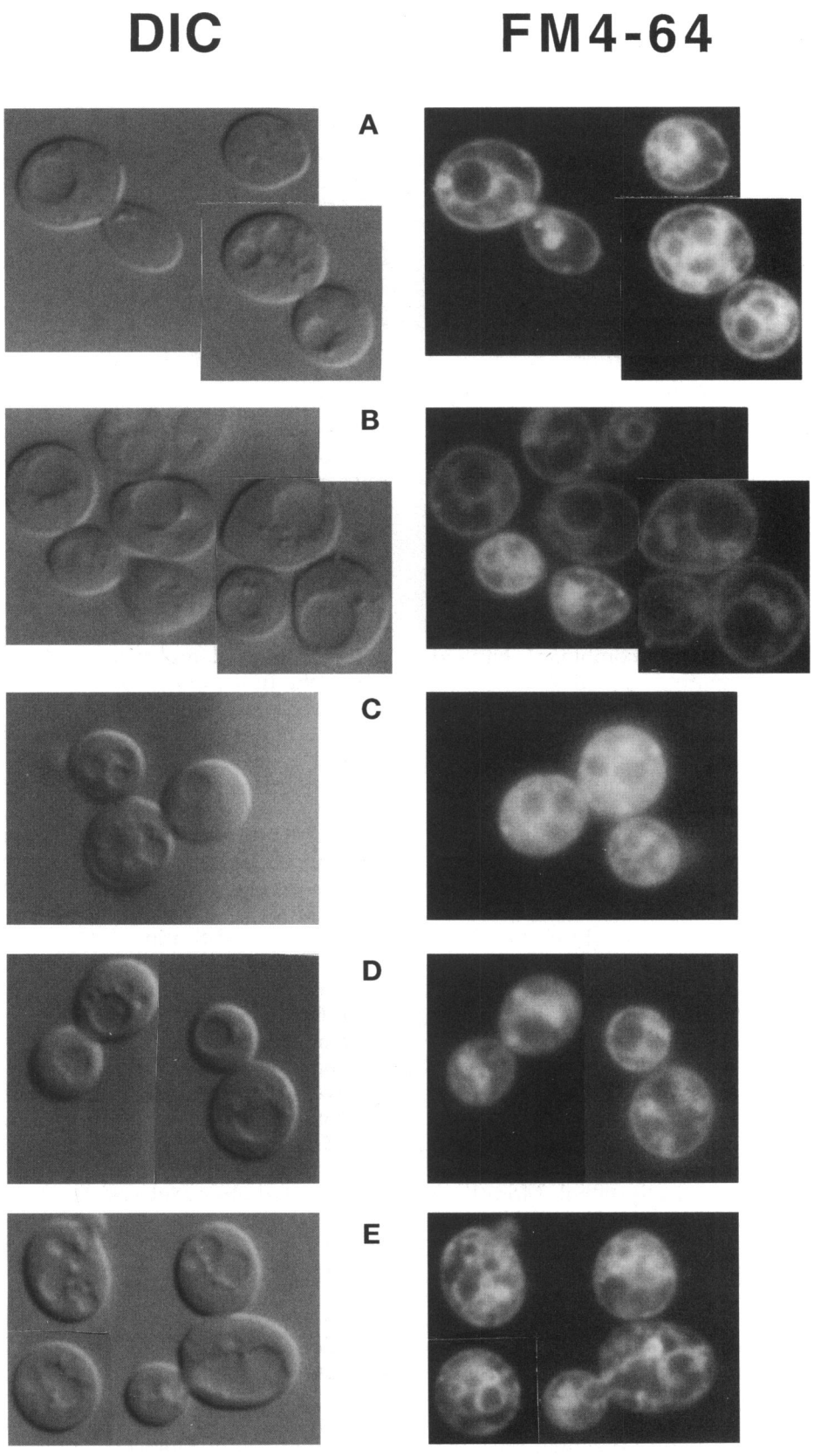
DIC
FM4-64
A
B
C
D
E

Table 2. Synthetic enhancement between *arp2-1* and *end3-1* mutations

Spore genotype	Normal growth	Temperature sensitive	Inviable
arp2-1 end3-1	0	5[a]	38
arp2-1 END3	0	30	1
ARP2 end3-1	0	30	1
ARP2 END3	43	0	0

[a] These spores germinated but all showed reduced growth and had temperature-sensitive thresholds between 24°C and 34°C, lower than either single mutant.

Table 3. Synthetic enhancement between *arp2-1* and *end4-1* mutations

Spore genotype	Normal growth	Temperature sensitive	Inviable
arp2-1 end4-1	0	34 (10[a])	11
arp2-1 END4	0	30	1
ARP2 end4-1	0	30	1
ARP2 END4	37	0	0

[a] Ten of 34 spores germinated but showed reduced growth and had temperature-sensitive thresholds between 24°C and 34°C, lower than either single mutant.

arp2–1 Displays Synthetic Lethality with end3–1

Testing of synthetic enhancement between various mutant alleles of actin cytoskeleton components has revealed a number of genetic interactions (Holtzman *et al.*, 1994). We tested whether synthetic enhancement could be observed between the *arp2–1* allele and the *end3–1* or *end4–1* alleles, both of which are deficient in the internalization step of endocytosis and actin organization at nonpermissive temperatures (Raths *et al.*, 1993). We looked for synthetically enhanced or lethal interaction by analyzing the recombinant haploid spores issued from the mating of YMW82 (*arp2–1*) with RH266–1D (*end3–1*) and RH268–1C (*end4–1*) strains. Doubly heterozygous diploids of *arp2–1* with either *end3–1* or *end4–1* did not show any growth or morphological phenotypes. Diploid strains were sporulated and haploid segregants dissected. Germination was about 90% as was the case in control crosses of each mutant with the opposite wild type. Tetrads were considered informative when the genotype of the complete tetrad could be determined after complementation tests with both singly mutant haploid strains. Thus, it could be ascertained which dead spores were *end arp2–1* double mutants. A synthetic quasilethal enhancement between *arp2–1* with *end3–1* was observed (Table 2). The few viable mutant *end3 arp2–1* spores (5/43) were severely growth impaired even at the permissive temperature and died at temperatures between 25 and 34°C when repicked from the germination plates. Although *end4* and *end3* mutations have essentially the same phenotype, *arp2–1* and *end4–1* were not synthetically lethal. More than half of the doubly mutant spores were viable with apparently normal growth (Table 3). The *arp2–1* and *end4–1* mutations do, however, show mild synthetic enhancement since the double mutation is more severe than either single mutation. Given that these three proteins are endocytosis deficient, the genetic data can be taken to indicate a functional interaction between Arp2p and End3p and to suggest that Arp2p and End4p may interact, whether directly or indirectly. Other means of evaluating potential *arp2* and *end* interactions, currently under investigation, should help us to determine whether the increased lethality of the combined mutations observed is indicative of physical interactions.

DISCUSSION

The essential yeast gene *ARP2* encodes a component of the actin cytoskeleton. A thermosensitive *arp2–1* mutant displays a disorganized actin cytoskeleton at nonpermissive temperature (Moreau *et al.*, 1996). Given the function of many components of the actin cytoskeleton in the exocytic and endocytic pathways, we investigated whether Arp2p could be involved in these processes.

When grown at permissive temperature, the *arp2–1* mutant shows ultrastructural organization very similar to that of wild type. Longer incubation at restrictive temperature resulted in the accumulation of vesicles in some cells of a heterogeneous population. After 2 h at restrictive temperature half of the cells showed no modification, whereas only 10% cells accumulated a large number of vesicles. This is different from the pattern we and others (Novick and Botstein, 1985; Goodson *et al.*, 1996) observed in *act1–3* cells. Even at permissive temperature some *act1–3* cells accumulate vesicles and the onset of a more severe defect was visible after short-term incubation at the restrictive temperature, with vesicles accumulated in the bud (Goodson *et al.*, 1996). After a 1-h incubation at 37°C, we observed that the majority of *act1–3* cells accumulated abundant vesicles that correlated with a defect in plasma membrane delivery of uracil permease. In contrast, *arp2–1* cells did not display defective cell surface delivery of either periplasmic invertase or uracil permease. Therefore, it seems likely that accumulation of vesicles may be a late and/or secondary effect of the *arp2–1* mutation. Moreover, because viability of *arp2–1* mutant cells begins to fall off after 2 h at the restrictive temperature (Moreau *et al.*, 1996), we cannot completely exclude the possibility that vesicle accumulation represents a terminal phenotype.

Whereas the exocytic pathway does not appear strongly affected in the *arp2–1* mutant, the defect in the endocytic process is striking. Our earlier observations of LY staining showed a drastic reduction in the amount of dye taken up by *arp2–1* cells at permissive and restrictive temperatures. This suggested an endocytic defect either in internalization or in subsequent steps of the endocytic pathway or in both events. We show herein that CPY was correctly delivered to the vacuole in *arp2–1* mutant cells. In good agreement with this result is the observation that the lipophilic dye FM 4–64, although taken up to a lesser extent in the mutant, transited through endosome-like membranous structures to the vacuolar membrane in a similar way in *arp2–1* and wild-type cells. Thus, by these criteria, *arp2–1* cells show no evidence of a defect in transit from the plasma membrane to the vacuole after shift to the restrictive temperature. We therefore examined events at the plasma membrane more closely, using uracil permease as a reporter.

The *arp2–1* mutation provided strong protection against stress-induced permease degradation. Two independent observations allow us to conclude that the internalization step of endocytosis was blocked. First, the *arp2–1* mutation conferred strong protection against the loss of uracil uptake (due to plasma membrane located permease) normally observed in wild-type cells in response to different stress conditions. Second, mutant cells showed abnormal accumulation of ubiquitinated forms of uracil permease that appear prior to internalization. A similar fate of uracil permease was observed in *act1–3* cells, strongly defective for permease internalization (Galan *et al.*, 1996). Similar ubiquitinated derivatives of Ste2p (Hicke and Riezman, 1996), Ste3p (Roth and Davis, 1996), or Ste6p (Egner and Kuchler, 1996; Kölling and Hollenberg, 1994) were reported to accumulate in *end4–1* mutant cells, defective for the internalization step of endocytosis. Not only is the alteration in endocytosis immediate in *arp2–1* cells placed at the restrictive temperature, but uracil permease internalization is already defective in mutant cells grown at permissive temperature, as was seen for LY accumulation. We had previously observed a similar alteration in the internalization step of endocytosis in the *act1–3* mutant at 24°C with the uracil permease system (Galan *et al.*, 1996), in agreement with the defect in LY uptake (Kübler and Riezman, 1993).

In view of these results, we conclude that Arp2p is involved in the internalization step of endocytosis, as are a growing number of components of the actin cytoskeleton (Kübler and Riezman, 1993; Bénédetti *et al.*, 1994; Munn *et al.*, 1995; Tang and Cai, 1996; Wendland *et al.*, 1996). The synthetically lethal interaction we found between *end3–1* and *arp2–1* mutations suggests interaction between Arp2p and End3p, although the mechanism of interaction is unknown. Both components are essential for the internalization step of endocytosis (as is End4p/Sla2p) but whether their interaction is direct or involves another protein in a complex or whether both participate in a common biochemical function necessary for internalization has not been determined. End3p has been postulated to function in the control of cortical patches size (Bénédetti *et al.*, 1994). The *END3* gene has been reported as a multicopy suppressor of the *pan1–4* mutation, which also disorganizes the actin cytoskeleton. Pan1p, like End3p and Arp2p, localizes to actin patches (Tang and Cai, 1996). Interestingly, both End3p and Pan1p were reported to carry an EH domain, which has been reported to be involved in protein–protein interactions (Tang and Cai, 1996). Sla2p/End4p has also been found to control the assembly of the cortical cytoskeleton (Holtzman *et al.*, 1993) and synthetic lethality was also reported for Sla2p/End4p and Act1p (as well as for Act1p and Sac6p; Holtzman *et al.*, 1994). The fact that Arp2p colocalizes with actin in patches and *arp2–1 end3–1* and *arp2–1 end4–1* synthetic enhancement results are consistent with the hypothesis of Arp2p being important for the structure or maintenance of actin patches. This could be via an effect on the polymerization of actin filaments although we have to date not been able to demonstrate direct interaction between Arp2p and Act1p (Madania and Winsor, unpublished results). Alternatively, Arp2p could also be implicated in actin-patch–membrane interaction and/or actin-patch–actin cables interaction according to the model of Mulholland *et al.* (1994). Whether Arp2p interacts directly with End3p and/or End4p and whether it functions in one or several different functional complex(es) of actin patches remains to be determined.

The question has been raised whether the disorganization of the cytoskeleton is the origin or the consequence of defective internalization (Bénédetti *et al.*, 1994). Certain cytoskeletal mutants including *abp1*Δ, *pfy1*Δ (profilin), *myo2–66* (myosin type V), and *tpm1*Δ (tropomyosin) appear normal for endocytosis (Kübler and Riezman, 1993; Kübler *et al.*, 1994; Munn *et al.*, 1995). Moreover, the endocytosis deficiency in the *arp2–1* mutant is readily detected at permissive temperature in conditions where actin patches show normal polarized organization. Clearly, impaired endocytosis in this case is not a direct consequence of overall actin disorganization as revealed by staining of actin filaments. This observation suggests that less visible subcellular structures (complexes) involved in the internalization step of endocytosis might exist that are impaired at 25°C in *arp2–1* without visible effects on the polarized organization of patches.

Phenotypes displayed by the *arp2–1* mutant are similar to *act1* phenotypes, with the exception of effects on the exocytic pathway. Vesicle accumulation in the *arp2–1* mutant was much more limited than that ob-

served for the *act1–3* mutant. Since many of the same processes appear to be affected in *arp2–1* and *act1* mutants, Arp2p appears to be implicated in major functions of the actin network. In particular, to our knowledge this is the first report of an actin-related protein being involved in endocytosis. In conclusion, these results and our previous characterization of the *arp2–1* mutant (Moreau *et al.*, 1996) indicate that Arp2p interacts with cellular complexes necessary for actin functions but do not exclude the possibility that Arp2p may also interact with other cellular complexes.

ACKNOWLEDGMENTS

We thank R. Martin for his interest in this work and C. Volland and D. Urban-Grimal for critical reading of the manuscript. We are indebted to M.-R. Chevallier, R. Jund, H. Riezman, and R. Serrano for providing antisera and to P. Hieter, P. Novick, H. Riezman, R. Scheckman, T. Stevens, F. Kepes, and M. Hochstrasser for generously providing strains and plasmids. This work was funded by the Centre National de la Recherche Scientifique and the Université Louis Pasteur, Strasbourg. V.M. was supported by a thesis scholarship from the Association pour la Recherche sur le Cancer, and J.-M.G. was supported by a thesis scholarship from the Ministèfre de l'enseignement supérieur et de la Recherche.

REFERENCES

Adams, A.E.M., and Pringle, J.R. (1984). Relationship of actin and tubulin distribution to bud growth in wild-type and morphogenetic-mutant *Saccharomyces cerevisiae*. J. Cell Biol. *98*, 934–945.

Bénédetti, H., Raths, S., Crausaz, F., and Riezman, H. (1994). The *END3* gene encodes a protein that is required for the internalization step of endocytosis and for actin cytoskeleton organization in yeast. Mol. Biol. Cell *5*, 1023–1037.

Carlson, M., and Botstein, D. (1982). Two differentially regulated mRNAs with different 5′ ends encode secreted and intracellular forms of yeast invertase. Cell *28*, 145–154.

Cleves, A.E., Novick, P.J., and Bankaitis, V.A. (1989). Mutation in the *SAC1* gene suppress defects in yeast Golgi and yeast actin functions. J. Cell Biol. *109*, 2939–2950.

Davis, N.G., Horecka, J.L., and Sprague, J.G.F. (1993). Cis- and trans-acting functions required for endocytosis of the yeast pheromone receptors. J. Cell Biol. *122*, 53–65.

Donnelly, S.F.H., Pocklington, M.J., Pallotta, D., and Orr, E. (1993). A proline-rich protein, verprolin, involved in cytoskeletal organization and cellular growth in the yeast *Saccharomyces cerevisiae*. Mol. Microbiol. *10*, 585–596.

Drubin, D.G. (1991). Development of cell polarity in budding yeast. Cell *65*, 1093–1096.

Ecker, D.J., Ishaq Khan, M., Marsh, J., Butt, T.R., and Crooke, S.T. (1987). Chemical synthesis and expression of a cassette adapted ubiquitin gene. J. Biol. Chem. *262*, 3524–3527.

Egner, R., and Kuchler, K. (1996). The yeast multidrug transporter Pdr5 of the plasma membrane is ubiquitinated prior to endocytosis and degradation in the vacuole. FEBS Lett. *378*, 177–181.

Field, C., and Schekman, R. (1980). Localized secretion of acid phosphatase reflects the pattern of cell surface growth in *Saccharomyces cerevisiae*. J. Cell Biol. *86*, 123–128.

Galan, J.M., Moreau, V., André, B., Volland, C., and Haguenauer-Tsapis, R. (1996). Ubiquitination mediated by the Npi1p/Rsp5p ubiquitin-protein ligase is required for endocytosis of the yeast uracil permease. J. Biol. Chem. *271*, 10946–10952.

Geli, M.I., and Riezman, H. (1996). Role of type I myosins in receptor-mediated endocytosis in yeast. Science *272*, 533–535.

Gietz, D., St Jean, A., Woods, R.A., and Schiestl, R.H. (1992). Improved method for high efficiency transformation of intact yeast cells. Nucleic Acids Res. *20*, 1425.

Goldstein, D., and Lampen, J. (1975). Beta-D-fructofuranoside fructohydrolase from yeast. Methods Enzymol. *42*, 504–511.

Goodson, H.V., Anderson, B.L., Warrick, H.M., Pon, L.A., and Spudich, J.A. (1996). Synthetic lethality screen identifies a novel yeast myosin I gene (*MYO5*): myosin I proteins are required for polarization of the actin cytoskeleton. J. Cell Biol. *133*, 1277–1291.

Govindan, B., Bowser, R., and Novick, P. (1995). The role of Myo2, a yeast class V myosin, in vesicular transport. J. Cell Biol. *128*, 1055–1068.

Graham, T.R., and Emr, S. (1991). Compartmental organization of Golgi-specific protein modification and vacuolar protein sorting events defined in a yeast *sec18* (NSF) mutant. J. Cell Biol. *114*, 207–218.

Harsay, E., and Bretscher, A. (1995). Parallel secretory pathways of the cell surface in yeast. J. Cell Biol. *131*, 297–310.

Hein, C., Springael, J.-Y., Volland, C., Haguenauer-Tsapis, R., and André, B. (1995). *NPI1*, an essential yeast gene involved in induced degradation of Gap1 and Fur4 permeases, encodes the Rsp5 ubiquitin-protein ligase. Mol. Microbiol. *18*, 77–87.

Hicke, L., and Riezman, H. (1996). Ubiquitination of a yeast plasma membrane receptor signals its ligand-stimulated endocytosis. Cell *84*, 277–287.

Hochstrasser, M., Ellison, M.J., Chau, V., and Varshavsky, A. (1991). The short-lived MATα2 transcriptional regulator is ubiquitinated in vivo. Proc. Natl. Acad. Sci. USA *88*, 4606–4610.

Holtzman, D.A., Wertman, K.F., and Drubin, D.G. (1994). Mapping actin surfaces required for functional interactions in vivo. J. Cell Biol. *126*, 423–432.

Holtzman, D.A., Yang, S., and Drubin, D.G. (1993). Synthetic-lethal interactions identify two novel genes, *SLA1* and *SLA2*, that control membrane cytoskeleton assembly in *Saccharomyces cerevisiae*. J. Cell Biol. *122*, 635–644.

Jansen, R.-P., Dowzer, C., Michaelis, C., Galova, M., and Nasmyth, K. (1996). Mother cell-specific HO expression in budding yeast depends on the unconventional myosin Myo4p and other cytoplasmic proteins. Cell *84*, 687–697.

Johnston, G.C., Prendergast, J.A., and Singer, R.A. (1991). The *Saccharomyces cerevisiae MYO2* gene encodes an essential myosin for vectorial transport of vesicles. J. Cell Biol. *113*, 539–551.

Julius, D., Schekman, R., and Thorner, J. (1984). Glycosylation and processing of pre-pro-α-factor through the yeast secretory pathway. Cell *36*, 309–318.

Jund, R., Weber, E., and Chevallier, M.R. (1988). Primary structure of the uracil transport protein of *Saccharomyces cerevisiae*. Eur. J. Biochem. *171*, 417–424.

Kelleher, J.F., Atkinson, S.J., and Pollard, T.D. (1995). Sequences, structural models and cellular localization of the actin-related proteins Arp2 and Arp3 from *Acanthamoeba*. J. Cell Biol. *131*, 385–397.

Kölling, R., and Hollenberg, C.P. (1994). The ABC-transporter Ste6 accumulates in the plasma membrane in a ubiquitinated form in endocytosis mutants. EMBO J. *13*, 3261–3271.

Kübler, E., and Riezman, H. (1993). Actin and fimbrin are required for the internalization step of endocytosis in yeast. EMBO J. *12*, 2855–2862.

Kübler, E., Schimmöller, F., and Riezman, H. (1994). Calcium-independant calmodulin requirement for endocytosis in yeast. EMBO J. *13*, 5539–5546.

Lai, K., Bolognese, C.P., Swift, S., and McGraw, P. (1995). Regulation of inositol transport in *Saccharomyces cerevisiae* involves inositol-induced changes in permease stability and endocytic degradation in the vacuole. J. Biol. Chem. *270*, 2525–2534.

Liu, H., and Bretscher, A. (1992). Characterization of *TPM1* disrupted yeast cells indicates an involvement of tropomyosin in directed vesicular transport. J. Cell Biol. *118*, 285–299.

Machesky, L.M., Atkinson, S.J., Ampe, C., Vandekerckhove, J., and Pollard, T.D. (1994). Purification of a cortical complex containing two unconventional actins from *Acanthamoeba* by affinity chromatography on profilin-agarose. J. Cell Biol. *127*, 107–115.

Moreau, V., Madania, A., Martin, R.P., and Winsor, B. (1996). The *Saccharomyces cerevisiae* actin-related protein Arp2 is involved in the actin cytoskeleton. J. Cell Biol. *134*, 117–132.

Mulholland, J., Preuss, D., Moon, A., Wong, A., Drubin, D., and Botstein, D. (1994). Ultrastrusture of the actin cytoskeleton and its association with the plasma membrane. J. Cell Biol. *125*, 381–391.

Munn, A.L., Stevenson, B.J., Geli, M.I., and Riezman, H. (1995). *end5, end6, end7*: mutations that cause actin delocalization and block the internalization step of endocytosis in *Saccharomyces cerevisiae*. Mol. Biol. Cell *6*, 1721–1742.

Nelson, K.K., Holmer, M., and Lemnon, S. (1996). *SCD5*, a suppressor of clathrin deficiency, encodes a novel protein with a late secretory function in yeast. Mol. Biol. Cell *7*, 245–260.

Novick, P., and Botstein, D. (1985). Phenotypic analysis of temperature-sensitive yeast actin mutants. Cell *40*, 405–416.

Novick, P., Field, C., and Schekman, R. (1980). Identification of 23 complementation groups required for post-translational events in the yeast secretory pathway. Cell *21*, 205–215.

Novick, P., Osmond, B.C., and Botstein, D. (1989). Suppressors of yeast actin mutations. Genetics *121*, 659–674.

Novick, P., and Schekman, R. (1979). Secretion and cell-surface growth are blocked in a temperature-sensitive mutant of *Saccharomyces cerevisiae*. Proc. Natl. Acad. Sci. USA *76*, 1858–1862.

Raths, S., Rohrer, J., Crausaz, F., and Riezman, H. (1993). *end3* and *end4*: two mutants defective in receptor-mediated and fluid-phase endocytosis in *Saccharomyces cerevisiae*. J. Cell Biol. *120*, 55–65.

Riballo, E., Herweijer, M., Wolf, D.H., and Lagunas, R. (1995). Catabolite inactivation of the yeast maltose transporter occurs in the vacuole after internalization by endocytosis. J. Bacteriol. *177*, 5622–5627.

Riezman, H. (1993). Yeast endocytosis. Trends Cell Biol. *3*, 273–277.

Roth, A.F., and Davis, N.G. (1996). Ubiquitination of the yeast a factor receptor. J. Cell Biol. *134*, 661–674.

Sachs, A.B., and Deardoff, J.A. (1992). Translation initiation requires the PAB-dependent poly(A) ribonuclease in yeast. Cell *70*, 961–973.

Sachs, A.B., and Deardoff, J.A. (1995). Cell *83*, 1059 (erratum.).

Schekman, R., and Novick, P. (1982). The secretory process and yeast cell surface assembly. In: The Molecular Biology of the Yeast *Saccharomyces* (Metabolism and Gene Expression), ed. J.V. Strathern, E.W. Jones, and J.R. Broach, Plainview, NY: Cold Spring Harbor Laboratory Press.

Schwob, E., and Martin, R.P. (1992). New yeast actin-like gene required late in the cell cycle. Nature *355*, 179–182.

Singer, B., and Riezman, H. (1990). Detection of an intermediate compartment involved in transport of alpha-factor from the plasma membrane to the vacuole in yeast. J. Cell Biol. *110*, 1911–1922.

Sivadon, P., Bauer, F., Aigle, M., and Crouzet, M. (1995). Actin cytoskeleton and budding pattern are altered in the yeast *rvs161* mutant: the Rvs161 protein shares common domains with the brain protein amphiphysin. Mol. Gen. Genet. *246*, 485–495.

Tang, H.-Y., and Cai, M. (1996). The EH-domain-containing protein Pan1 is required for normal organization of the actin cytoskeleton in *Saccharomyces cerevisiae*. Mol. Cell. Biol. *16*, 4897–4914.

Tschopp, J., Esmon, P.C., and Schekman, R. (1984). Defective plasma membrane assembly in yeast secretory mutants. J. Bacteriol. *160*, 966–970.

Vida, T.A., and Emr, S. (1995). A new vital stain for visualizing vacuolar membrane dynamics and endocytosis in yeast. J. Cell Biol. *128*, 779–792.

Vida, T.A., Huyer, G., and Emr, S.D. (1993). Yeast vacuolar proenzymes are sorted in the late Golgi complex and transported to the vacuole via a prevacuolar endosome-like compartment. J. Cell Biol. *121*, 1245–1256.

Volland, C., Garnier, C., and Haguenauer-Tsapis, R. (1992). In vivo phosphorylation of the yeast uracil permease. J. Biol. Chem. *267*, 23767–23771.

Volland, C., Urban-Grimal, D., Geraud, G., and Haguenauer-Tsapis, R. (1994). Endocytosis and degradation of the yeast uracil-permease under adverse conditions. J. Biol. Chem. *269*, 9833–9841.

Welch, M.D., Holtzman, D.A., and Drubin, D.G. (1994). The yeast actin cytoskeleton. Curr. Opin. Cell Biol. *6*, 110–119.

Wendland, B., McCaffery, J.M., Xiao, Q., and Emr, S. (1996). A novel fluorescence-activated cell sorter-based screen for yeast endocytosis mutants identifies a yeast homologue of mammalian eps15. J. Cell Biol. *135*, 1485–1500.